FATIGUE CRACK PROPAGATION IN WELDED JOINTS OF THE STEEL CA6NM WITHOUT POS WELDING HEAT TREATMENT

Anderson Geraldo Marenda Pukasiewicz
Unidade de Ponta Grossa do CEFET-PR, Ponta Grossa - PR
ander@pg.cefetpr.br

Nilceu Novicki
Unidade de Medianeira do CEFET-PR, Medianeira - PR
nilceu@yahoo.com

Sérgio Luiz Henke
Instituto de Tecnologia para o Desenvolvimento LACTEC, Curitiba - PR
henke@lactec.org.br

Walter Jesus Paucar Casas
UFRGS, Departamento de Engenharia Mecânica, Rua Sarmento Leite 425, CEP 90050-170, Porto Alegre - RS
walter.paucar.casas@ufrgs.br

Abstract. *The soft martensitic stainless steel, used in hydraulic turbines and the petrochemical industry, shows one adequate resistance to the erosion, cavitation and a good weldability, but shows restrictions with reference to the fatigue strength and fracture in the weld metal and the heat affected zone. The purpose of this work is to evaluate the behavior of the fatigue crack propagation in welded joints with this steel. Additionally, the fracture mechanisms are evaluated after the rupture with scanning electron microscopy. The fatigue crack growth was realized with compact tension specimens, with insertion of the pre-crack in the weld metal, the heat affected zone and the base metal; the microhardness profile and metallography. Initial results on different regions of the joint without post weld heat treatment indicate that the constants C and m of the base metal are 1,22x10-8 and 2,62 respectively, while for the heat-affected zone, they are 7,83x10^{-11} and 3,82, and for the weld metal, they are 2,47x10^{-10} and 3,80. Variations in the fracture mechanisms for all levels of ΔK were verified. These results plus those with post weld heat treatment will be used for modeling the fracture and fatigue in welded joints with this material.*

Keywords: *fracture mechanisms, fatigue, welding, martensitic stainless steel, welded joints.*

1. Introduction

Since 60´th decade the soft martensitic stainless steels have been used in hydraulic turbines and the petrochemical industry; for example, these steels contain 12 - 13% of chrome, 2 - 5% of nickel and less than 0,06% of carbon in the construction of hydraulic turbines (Bilmes et all, 2000). These steels have high yield strength, excellent toughness, adequate resistance to cavitation and good weldability. Martensitic stainless steels with low carbon content, such as the CA6NM steel, are always quenched and tempered. The excellent toughness occurs because the formation of a finely dispersed austenite as result of the intercritical tempering in temperatures close to 600°C (Folkhard, 1988).

In soft martensitic steels the carbon content is kept below 0,1% in mass to improve weldability by promoting a structure with fewer tendency for cold cracking, better corrosion resistance, and better toughness; the weld metal (WM) and the heat affected zone (HAZ) have lower impact resistance and fracture toughness than the CA6NM alloy. In general, welded structures show inferior behavior compared to the base metal (BM) because the welding process involves many modifications in the microstructure with the creation of harder and brittle microstructures (Akhtar and Brodie, 1979 and Bilmes et all, 2000).

Fatigue tests are extensively used to evaluate the dynamic behavior of materials; however these tests are more used in samples with homogeneous material. For determining the fatigue behavior of welded joints, the study and the control of the tests are more complex, because welded joints involve microstructural variations in small distances, and contain complex distributions of residual stresses. Then, a more detailed study of the fatigue behavior of welded joints is necessary for evaluating the resistance in welded structures (Moltubakk, 1999).

Nowadays, the fatigue and fracture tests are accomplished in agreement with standards and codes developed by several institutions such as the American Society for Testing and Materials (ASTM) and the British Standards Institution (BSI). These tests were originally developed for use in homogeneous samples, and they are based over the curves *S-N*, ε-*N* and *da*/*dN*-ΔK for fatigue evaluation (Moltubakk, 1999).

The fatigue crack growth rates during the period of stable crack propagation can be described by the empirical power law relationship as proposed by Paris and Erdogan, given by Eq. (1).

$$\frac{da}{dN} = C\,\Delta K^{m} \tag{1}$$

where da/dN is the fatigue crack growth rate, ΔK is the stress intensity factor range, C and m are constants of the material involving testing conditions such as environment, frequency, temperature and stress ratio R. (Hertzberg, 1996).

The purpose of this work is to study the fatigue crack propagation of welded joints with the CA6NM steel (BM, HAZ and WM) without pos-weld heat treatment (PWHT) as well as to identify the fracture mechanisms.

2. Experimental procedures

The employed material has been the soft martensitic stainless steel CA6NM, austenitized at 1050 ºC and air quenched and tempered at 580 ºC. The chemical composition of the steel, in weight percentage, was 0,020 C, 0,64 Mn, 12,40 Cr, 3,70 Ni, 0,42 Mo, 0,008 P and 0,0018 S. The steel has yield strength of 666 MPa and tensile strength of 799 MPa.

The dimensions of the welded bars were 200x70x20 mm, with fillet of 40° in a K joint. The welding process was manual MIG and the composition of the tubular electrode AWS ER 410 (ϕ 1,6mm) used in weight percentage was 0,026 C, 0,33 Mn, 10,50 Cr, 3,60 Ni, 0,45 Mo, 0,019 P and 0,0084 S. The welding parameters were: 25,6 V, 320 A, heat input of about 18,2 kJ/cm, pre-heating temperature of 150°C and interpass temperature between 150 and 180°C, shielding gas was 92% Argon with 8% of CO_2. Metallographic observations and microhardness measurements were made to identify different regions in a welded joint. To study fatigue crack growth rate in different regions of the welded joint was used the compact tension (CT) samples that were aligned parallel to the welding direction, as shown in Fig. (1).

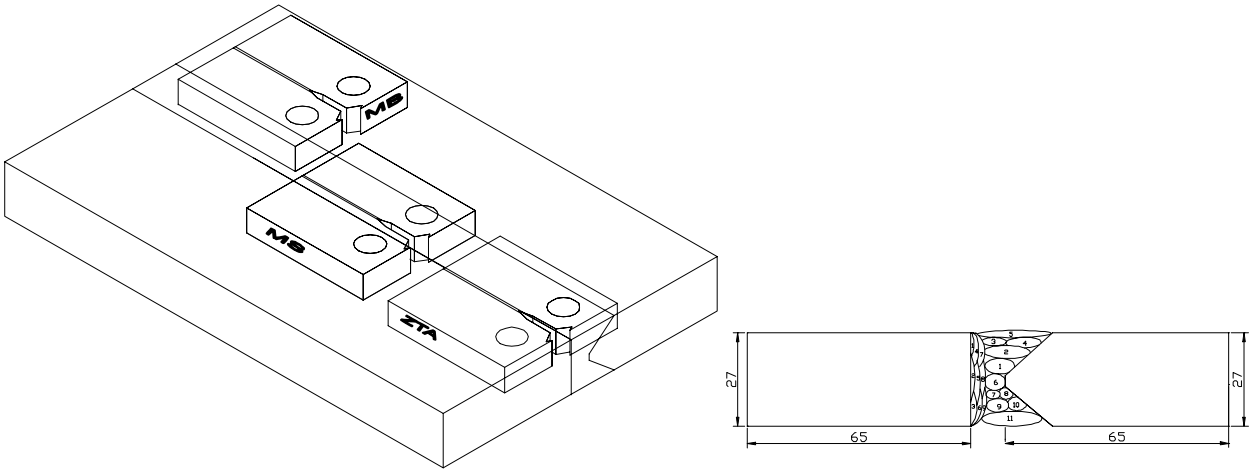

Figure 1. Disposition of samples in the welded joint.

The fatigue crack growth tests were accomplished in agreement with the standard ASTM E647-95 in a dynamic testing machine, Instron model 8500 Plus, with servo-hydraulic actuator at room temperature. The used frequency was 20 Hz, with constant amplitude of the sinusoidal waveform, and the applied stress ratio (R) was equal to 0,1 through the test, and the crack measurement was realized with a crack opening displacement gage.

Fatigue crack growing tests were realized in CT testing bodies. In order to restrict the direction of crack growing, a 90°V-notch of 0,5 mm depth was machined on the opposite surfaces of all CTs specimens. The dimensions of the CT testing body was machined in agreement with orientations of the standard ASTM E647-95, Fig. (2), where W is equal to 51,16 mm. After rupture, the samples were examined by a Phiplips XL30 scanning electron microscope (SEM) for the identification of the fracture mechanisms.

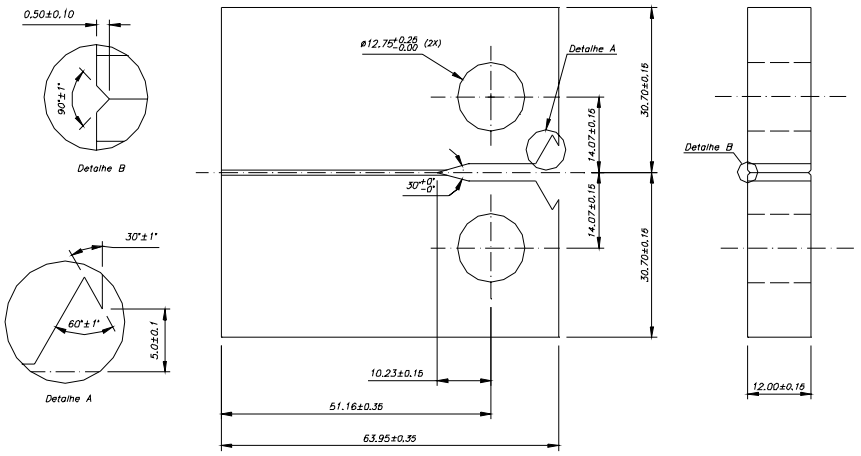

Figure 2. Dimensions of the CT specimen.

3. Results and discussion

It was verified that didn't occur grain growth near to the fusion line in the HAZ of the CA6NM steel without PWHT, this is due to the low temperature Ac_4 ($\gamma \leftrightarrow \delta$). The microstructure of the welded joint is shown in Fig. (3). This low temperature promotes refinement of the grain size close to the fusion line (Henke, 1998).

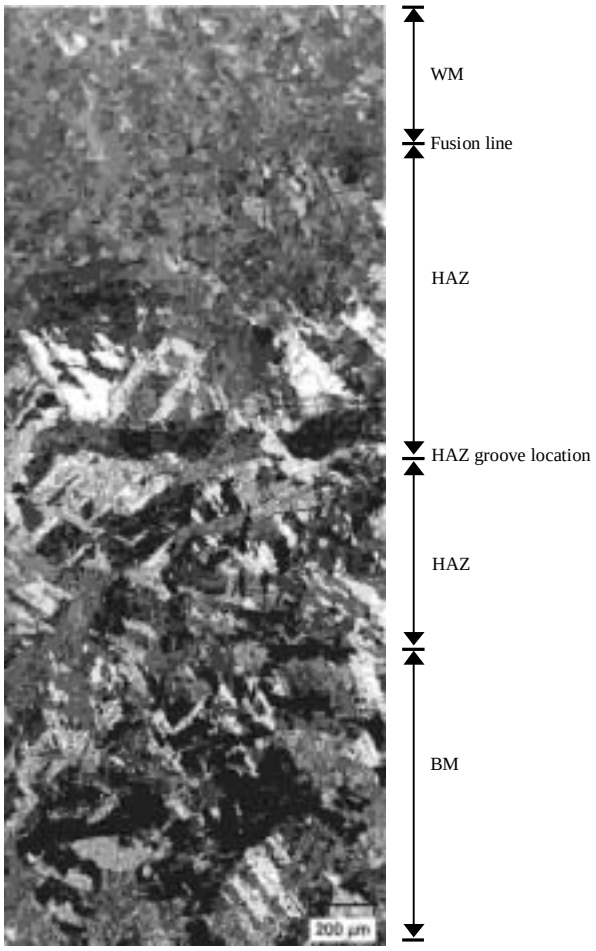

Figure 3. Micrographs of the joint as welded (Villela's etch, polarized light).

The variation of hardness in the weld is given in Fig. (4). It is found that the hardness drops suddenly from the WM to the HAZ and the BM. The hardness distribution indicates that the subsequent passes temper the martensite formed in the HAZ.

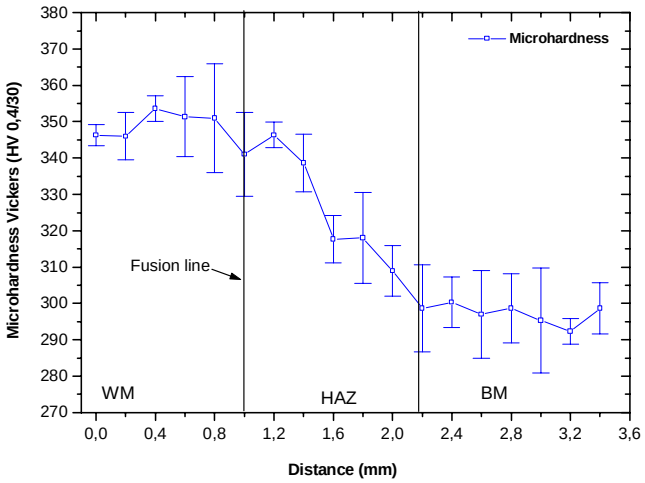

Figure 4. Hardness distribution in the joint as welded.

The fatigue crack growth, *da*/*dN*, versus stress intensity factor range, Δ*K*, in BM, HAZ and WM is shown in Fig. (5).

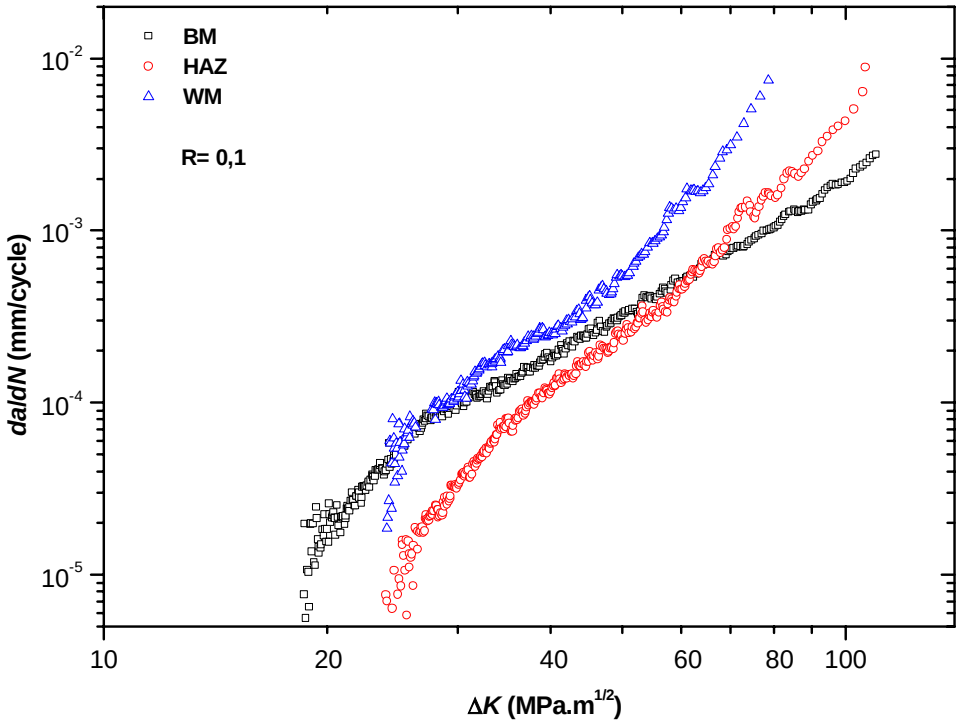

Figure 5. Fatigue crack growth of the welded joint of the CA6NM steel, without PWHT.

The Δ*P* constant amplitude testing is not indicated to measure fatigue crack growth rates lower than 10^{-5} mm/cycle and the ΔK_{th} presents high dispersion in their values and the analysis of the ΔK_{th} will not be realized in this work (ASTM, 1996 and Kang et all, 1990).

The residual stress superimposed on the applied stress can cause the crack-tip stress intensity factor be different from that computed solely from externally applied loads and the values of the real stress intensity factor is difficult to be analyzed, although the effect of residual stress would be lower in the relatively high Δ*K* range. (ASTM, 1996 and Tsay et all, 2001).

The residual stresses in welded joints are modified during the preparation of the samples and the pre-cracking, and change the analysis of its influence in fatigue crack growth rates (Arai et all, 1995; Beghini et all, 1994 and Shi et all, 1990).

For intermediate values of Δ*K* the samples have different behavior, with larger straight-line inclinations in the samples located in the HAZ and WM in relation with the BM. The inclination of the fatigue crack growth in the HAZ is larger than the BM, with crack growth rate lower than the BM until Δ*K* of approximately 62 MPa$\sqrt{m}$. Similar results are described in the literature (Lee et all, 2000 and Tsay et all, 2001). The smallest ductility of ZTA and WM might have

influenced the straight-line inclination, because the exponent *m* of the Paris Law tends to be larger for less ductile materials.

In relation to the samples located in the WM it was observed an increase in the straight-line inclination for a ΔK near to 45 MPa√m. This largest inclination for that ΔK value determines that the material showed a decrease in the resistance to the propagation of fatigue cracks. This change in inclination was accomplished with an alteration in fracture mechanisms in WM samples. The results of the constants *C* and exponential coefficient *m* of the Paris law, from these welded joints, with ΔK in MPa√m and da/dN in mm/cycle, are given in Tab. (1).

Table 1. Constants *C* and *m* for different regions of the welded joint.

Samples	***C***	***M***
WM	$2{,}470 \times 10^{-10}$	3,80
HAZ	$7{,}837 \times 10^{-11}$	3,82
BM	$1{,}224 \times 10^{-8}$	2,62

Figure 6 shows the fracture surface of BM, WM and HAZ samples for the low ΔK regime, therefore in the beginning of the fatigue crack growing curve. For these ΔK values the predominant fracture mechanism in the BM is fatigue striations highly facetted, and showing one small quantity of intergranular fracture, while for the HAZ and WM it is showed only facetted fatigue striations.

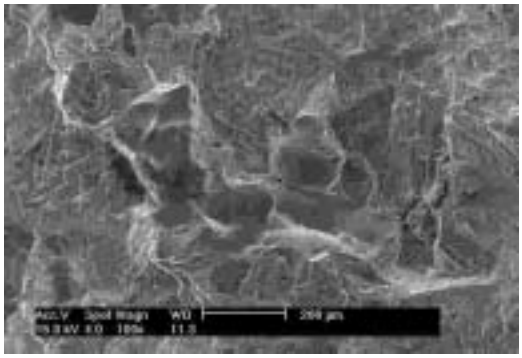
(a)

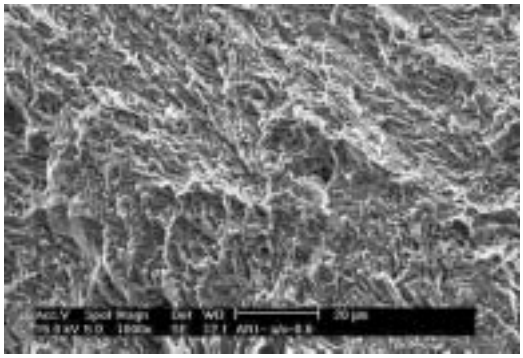
(b)

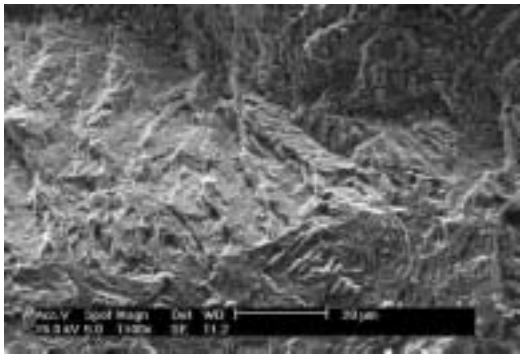
(c)

Figure 6. Fractography of BM (a), WM (b), for ΔK of 18 MPa√m and HAZ (c) with ΔK of 25 MPa√m.

The increase in the ΔK determines variations in the fracture mechanisms during the fatigue. For the CA6NM steel a transition was observed in the fracture for a ΔK of 21 MPa√m where the intergrained fracture was not verified, being found only fracture by striations. Variations in the fracture mechanisms were observed in WM for a ΔK of 30 MPa√m, where the formation of voids was verified in some areas, forming propagation planes. The sample located in the ZTA did not show any alteration in the fracture mechanism, remaining fatigue striations, Fig. (7).

For values of ΔK above 45 MPa√m is observed the formation of fatigue striations and secondary cracks in BM and HAZ, and for the samples located in WM is verified that the fracture mechanism is only by coalescement of voids. It is verified that the increase in the straight-line inclination can be associated to the fracture mechanism by coalescement of voids. The alteration in the fracture mechanism, and consequently, in the inclination of the straight line in WM might have occurred due to the crack growth in an area with high amount of scum inclusions, Fig. (8).

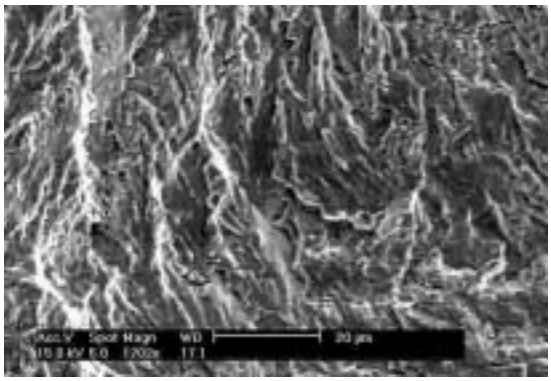
(a)

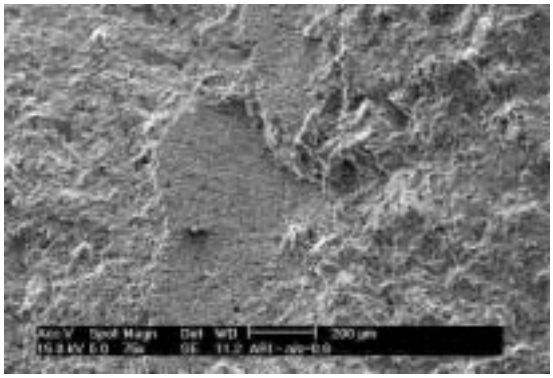
(b)

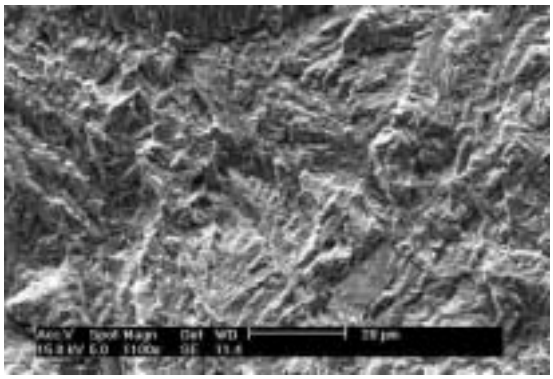
(c)

Figure 7. Fractography of BM (a), for Δ*K* of 21 MPa√m, WM (b), and HAZ (c) with Δ*K* of 30 MPa√m.

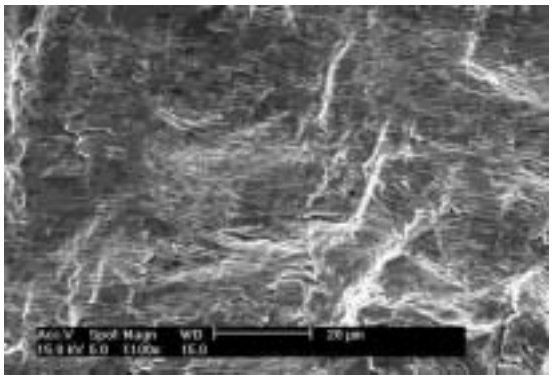
(a)

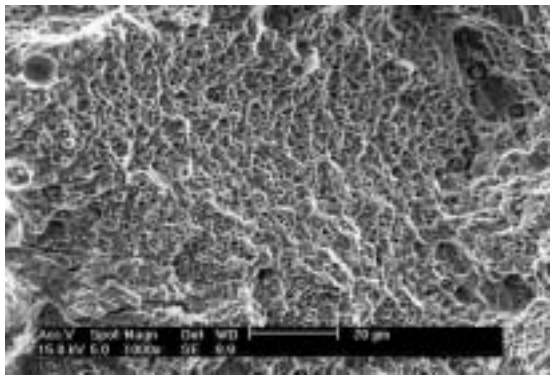
(b)

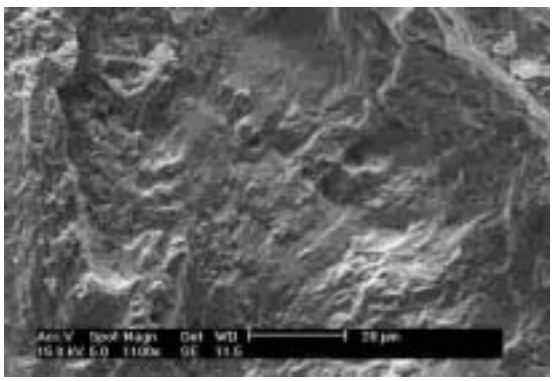
(c)

Figure 8. Fractography of BM (a), WM (b) and HAZ (c) for Δ*K* above of 45 MPa√m.

4. Conclusions

The tests of fatigue crack growth determined that the constants C and m of the BM are $1{,}224.10^{-8}$ and 2,63 respectively, being ΔK in MPa$\sqrt{}$m and da/dN in mm/cycle.

The fracture mechanisms observed in the base metal were intergrained and fatigue striations highly facetted, for low ΔK values, while fatigue striations were observed for intermediate and high ΔK values, with the presence of voids close of the rupture. The formation of plans of fatigue crack propagation by striations was observed in ZTA while the formation of plans of fatigue crack propagation by striations and fracture with coalescement of voids was observed in WM.

Scum existence kept in the solder strings influenced the fracture mechanisms and consequently the fatigue crack growth.

5. References

Akhtar, A., Brodie, N.W.,1979, "Field welding large turbine runners", Water Power & Dam Construction, September, 40-46.

Arai, Y., Hikuchi, M., Wtanabe, T., Nakagaki, M., 1995, "Residual stress due to welding and its effect on the assessment of cracks near the weld interface" International Journal of Pressure Vessel and Piping, 63, 237 – 248.

ASTM, 1996, "ASTM E647–95a: Standard test method for measurement of fatigue crack growth rates", ASTM E3 Vol 3.01 Metals-Mechanical Testing, Elevated and Low-Temperature Tests, Metallography, American Society for Testing and Materials.

Beghini, M., Bertini, L., Vitale E., 1994, "Fatigue crack growth in residual stress fields: experimental results and modeling", Fatigue Fract Engng Mater Struct, 17(12), 1433-1444.

Bilmes, P.D., Llorente, C.L., Pérez, I. J., 2000, "Toughness and microstructure of 13Cr4NiMo high strength steel welds", Journal of Materials Engineering and Performance, 09, 609-615.

Folkhard, E.,1988, "Welding Metallurgy of Stainless Steels", Springer-Verlag Wien New York.

Henke, S., 1998, "Desenvolvimento de procedimento de soldagem de aço inoxidável martensítico macio tipo CA6NM sem tratamento térmico posterior", Universidade Federal de Santa Catarina, Dissertação de Mestrado em Engenharia Mecânica, Florianópolis–SC, Brasil.

Hertzberg, R.W., 1996, "Deformation and fracture mechanics of engineering materials", John Wiley and Sons, 4th ed., New York.

Kang, K.J., Song, J.H., Earmme, Y.Y., 1990, "Fatigue crack growth and closure behavior through a compressive residual stress field", Fatigue Fract. Engng. Mater. Struct., 13, 1, 1-13.

Lee, H.K., Kim, K.S., Kim, C.M., 2000, "Fracture resistance of a steel weld joint under fatigue loading", Engineering Fracture Mechanics, 66, 403-419.

Moltubakk T.,1999, "Strength mismatch effects on the clivage fracture of the heat affected zone of steel welds", Norwegian University of Science and Technology, Department of Machine Design and Materials Technology, Ph.D. Thesis, Trondheim Norway, 112p.

Shi, Y.M., Chen, B.Y., Zhang, J.X., 1990, "Effects of welding residual stresses on fatigue crack growth behavior in butt welds of a pipeline steel", Eng Fract Mech, 36, 6, 893-902.

Tsay, L.W., Liu, C.C., Chao, Y.H., Shieh, Y.H., 2001, "Fatigue crack Propagation in 2,25 Cr- 1,0 Mo steel weldments in air and hydrogen", Materials Science and Engineering, A299, 16-26.